Braz J Phys (2015) 45:409–418
DOI 10.1007/s13538-015-0327-x

GENERAL AND APPLIED PHYSICS

Nonlinear Electromagnetic Waves in a Degenerate Electron-Positron Plasma

S. K. El-Labany[1] · W. F. El-Taibany[1,2] · A. E. El-Samahy[3] · A. M. Hafez[3] · A. Atteya[3]

Received: 10 February 2015 / Published online: 27 May 2015

Abstract Using the reductive perturbation technique (RPT), the nonlinear propagation of magnetosonic solitary waves in an ultracold, degenerate (extremely dense) electron-positron (EP) plasma (containing ultracold, degenerate electron, and positron fluids) is investigated. The set of basic equations is reduced to a Korteweg-de Vries (KdV) equation for the lowest-order perturbed magnetic field and to a KdV type equation for the higher-order perturbed magnetic field. The solutions of these evolution equations are obtained. For better accuracy and searching on new features, the new solutions are analyzed numerically based on compact objects (white dwarf) parameters. It is found that including the higher-order corrections results as a reduction (increment) of the fast (slow) electromagnetic wave amplitude but the wave width is increased in both cases. The ranges where the RPT can describe adequately the total magnetic field including different conditions are discussed.

Keywords Higher-order nonlinearity · Solitary waves · Relativistic effect · Degenerate pressure · Compact objects

✉ W. F. El-Taibany
eltaibany@hotmail.com; eltaibany@du.edu.eg

S. K. El-Labany
skellabany@hotmail.com; ellabany_s@du.edu.eg

A. E. El-Samahy
ahmedsamahy@yahoo.com

A. M. Hafez
am.hafez@sci.alex.edu.eg

A. Atteya
ahmed_ateya2002@yahoo.com

[1] Department of Physics, Faculty of Science, Damietta University, P.O. 34517, New Damietta, Egypt

[2] Department of Physics, College of Science for Girls in Abha, King Khalid University, P. O. 960, Abha, Saudi Arabia

[3] Department of Physics, Faculty of Science, Alexandria University, P. O. 21568, Alexandria, Egypt

1 Introduction

Since the early investigations of Bohm and Pines [1], major studies [2, 3] have been directed toward the study of physical properties of dense plasmas which are called *quantum plasmas*. Due to the significance of Pauli exclusion mechanism in such plasmas, rather distinct features such as quantum tunneling, degeneracy pressure, quantization of electronic density of states, and many other peculiar features [4] are expected to occur which are absent in the ordinary plasma. Such quantum effects can lead to distinct collective phenomena in quantum plasmas. Despite numerous applications of quantum plasmas in different areas such as semiconductors, nanotechnology, quantum optics, and electronics [5], there are many astrophysical situations such as white and brown dwarfs, neutron stars, and magnetars where quantum effects become dominant [6, 7].

A dense plasma can be described as a quantum fluid where its number density is so high that the electrons become degenerate and obey Fermi Dirac distribution. The study of a degenerate plasma has gained interest due to its existence in interstellar compact objects whose number densities lie in the range from 10^{25} to 10^{29} cm^{-3} [6–11] and in intense laser plasma experiments [12]. The quantum effect of degenerate plasmas becomes important when the

de-Broglie thermal wave length associated with the species (generally electrons) turns out to be equal or larger than the interparticle distance or the Fermi temperature (which depends on the particle number density) of the species becomes greater than the system thermal temperature [1, 6–8, 13, 14]. The degenerate plasma pressure in compact stars arises due to the combined effects of Pauli's exclusion and Heisenberg's uncertainty principles, which depends upon the number densities of the constituent particles but is independent of their own temperatures. The peculiarities of modeling nonlinear collective interactions in quantum plasmas have been pointed out recently [6, 7], where the essential physics and salient features of dense degenerate quantum plasmas are discussed. The study of electrostatic and electromagnetic perturbations with degenerate electron pressure under such extreme conditions of matter has recently been focused within the plasma physics community [15–21], with use of models concerning applications in astrophysical situations.

Whereas in an electron-ion (EI) plasma, the large mass difference among electrons and ions induces a significant disparity between relevant frequency and length scales, which can be exploited advantageously to disentangle some of the solitary wave characteristics. This is true not only for linear modes but also for nonlinear excitations. Among the most important types of nonlinear waves observed in EI plasmas is the ion acoustic (IA) wave. Using the reductive perturbation technique (RPT), Washimi and Taniuti [22] first studied the propagation of IA solitary waves that can be described by the Korteweg de Vries (KdV) equation. On the other side, a number of authors [23–26] have studied the nonlinear propagation of intense electromagnetic waves in electron-positron-ion (EPI) plasmas, in laboratory experiments [27–29], in fireballs producing gamma-ray bursts [30], and in solar flares [31]. In a warm EPI plasma at nonrelativistic temperatures, one has the possibility of existing acoustic-like waves [32]. Shukla et al. [16] stated that the electromagnetic pulses are associated with the compression of the plasma density and the wave magnetic field. In the electron-positron (EP) plasma, the solitary wave magnetic field pressure provides the restoring force, while the inertia comes from the equal mass electrons and positrons. The solitary pulses are formed due to a balance between the compressional wave dispersion arising from the curl of the inertial forces in Faraday's law and the nonlinearity associated with the divergence of the electron and positron fluxes, the nonlinear Lorentz forces, the advection of the EP fluids, and the nonlinear plasma current densities. Later, a strongly magnetized, ultradense EP plasma with degenerate electrons and positrons is considered by Khan et al. [33, 34]. They found that by introducing ion species in their EP model, the shear electromagnetic wave is shown to couple with electrostatic ion mode under certain conditions. Recently, the cosmic-ray positron fraction has been measured by Payload for Antimatter Matter Exploration and Light-nuclei Astrophysics (PAMELA) satellite [35–38]. The observed positron fraction rises in the energy range of 10–100 GeV, contrary to the prediction of secondary positrons, which are generated from cosmic-rays propagating in the interstellar medium. Over the last 5 years, several satellite and balloon observatories have suggested intriguing features in the cosmic ray lepton spectra [39, 40]. Kashiyama and Ioka [41] proved that white dwarf pulsars potentially could become TeV energy EP source based upon the energetics. Later on, Kashiyama et al. [42] stated that white dwarf pulsars can produce EP pairs and accelerate them up to TeV. Also, Kashiyama et al. [42] succeeded in explaining the reported excess of the EP flux in the range 100 GeV–1 TeV and the PAMELA positron excess. Serpico [43] has summarized the global picture emerging from the data, and some astrophysical diagnostics are also introduced.

To remove discrepancies between experimentally observed characteristics/space data of solitary wave solitons and theoretical predictions, various studies [44–49] have proved the necessity of including higher-order nonlinearity and dispersion in studying nonlinear plasma waves. The new soliton solutions are called "*dressed solitons*." For instance, Esfandyari-Kalejahi et al. [46] have studied the dressed electrostatic solitary excitations created in a three-component pair plasma. They observed that the higher-order nonlinearity leads to deformation of the soliton structure from bell-shaped to W-shaped depending on the variation in plasma parameter values. Chatterjee et al. [47] have studied the effects of positron concentration, electron-to-positron Fermi temperature ratio, and the soliton velocity on the amplitude and the width of the produced dressed soliton. Later, Akbari-Moghanjoughi [48] examined the possibility of propagation of bright- and dark-type solitary excitations by incorporating the higher-nonlinearity terms. Recently, Mehdipoor and Esfandyari-Kalejahi [49] proved that the higher-order corrections significantly change the properties of the KdV solitons propagating in an EPI plasma. However, all of these studies are only concerned with the electrostatic solitary wave solutions. To the best of our knowledge, no investigation has been made to examine the contribution of higher-order nonlinear and dispersion terms to electromagnetic excitations under extreme condition of matter which is the main motive of the present study. We consider a degenerate dense EP plasma model containing nonrelativistic, inertial ultracold electron and positron fluids. The mass ratio parameter is kept arbitrary to include an investigation for EI plasma model too. The basic equations describing our plasma system are presented in Section 2 . A KdV equation is derived, for the lowest-order perturbed magnetic field. The higher-order nonlinear and

dispersion effects are taken into account in the derivation of the inhomogeneous KdV type equation valid for the higher-order perturbed magnetic field. In Section 3, the renormalization method [50] is used to get the analytical stationary solutions of the two evaluation equations. A set of numerical illustrations along with a discussion related to white dwarfs application are provided in Section 4.

2 Basic Equations

The propagation of electromagnetic perturbations in a degenerate dense EP plasma system containing degenerate ultracold electron and positron fluids is considered. This plasma system is assumed to be immersed in an external static magnetic field ($\tilde{\mathbf{B}}_o$). Focusing on the propagation of the electromagnetic (transverse) perturbation modes ($\tilde{\nabla}\cdot\tilde{\mathbf{E}}=0$) in such a plasma medium is made. So, from Poisson's equation, we have $N_e = N_p = N$. The degenerate electron pressure (P_e), which is a function of electron density and thus approximately equals to the degenerate positron pressure ($P_p = P_e = P$), is assumed to be satisfied by the nonrelativistic degenerate equation of state [8]:

$$P=\frac{3}{5}\left(\frac{\pi}{3}\right)^{\frac{1}{3}}\frac{\pi\hbar^2}{m_e}N^{\frac{5}{3}}\simeq\frac{3}{5}\Lambda_c\hbar c N^{\frac{5}{3}},$$

where $\Lambda_c = \pi\hbar/m_e c = 1.2\times10^{-10}$ cm, $\hbar$ is the Planck constant divided by 2π, m_e is the mass of an electron, and c is the speed of light in vacuum. The dynamics of such electromagnetic perturbations in a degenerate EP plasma medium are described in normalized forms by[18]

$$\partial_t n+\partial_x\left(nu_x\right)=0, \tag{1}$$

$$d_t u_x+\frac{1}{2n}\partial_x\left(b_z^2+b_y^2\right)+\frac{3}{2}\beta\,\partial_x n^{\frac{2}{3}}=0, \tag{2}$$

$$d_t u_y-\mu\,d_t\left(\frac{1}{n}\partial_x b_z\right)-\frac{1}{n}b_x\partial_x b_y=0, \tag{3}$$

$$d_t u_z+\mu d_t\left(\frac{1}{n}\partial_x b_y\right)-\frac{1}{n}b_x\partial_x b_z=0, \tag{4}$$

$$\partial_t b_y+\partial_x\left(u_x b_y-u_y b_x\right)+\partial_x d_t u_z=0, \tag{5}$$

$$\partial_t b_z+\partial_x\left(u_x b_z-u_z b_x\right)-\partial_x d_t u_y=0, \tag{6}$$

where $d_t\,(=\partial_t+u_x\partial_x)$ is normalized by the reciprocal of the electron cyclotron frequency; $\omega_{ce}^{-1}\,[=m_e c/(eB_0)]$, $\vec{u}_j$ is the fluid velocity of j-plasma species (its components are $u_x, u_y,$ and u_z) normalized by $V_A[=B_o/\sqrt{4\pi n_0\left(m_e+m_p\right)}]$. $\beta=2\hbar c\Lambda_c n_o^{2/3}/\left[V_A^2\left(m_e+m_p\right)\right]$ and $n=N/n_o$, where n_o is the equilibrium value of N. The quantity m_p is the mass of positron species (it may be noted here that to pin-point the effect of the property of being equal mass of the plasma species, we will use $\mu=m_p/m_e$ instead of using $m_p/m_e=1$), $\tilde{\mathbf{b}}=\overrightarrow{\mathbf{B}}/B_o$. It was assumed that [18] (i) the perturbations propagate along the x-axis (i.e., $\tilde{\nabla}=\hat{\mathbf{e}}_x\partial/\partial x$), where $\hat{\mathbf{e}}_x$ is the unit vector along the x-axis, and (ii) the external magnetic field $\tilde{\mathbf{b}}$ lies in the $x-z$ plane (i.e., $\bar{\mathbf{b}}$ makes an angle θ with the x-axis). It may be remarked here that in this model, we concern with the electromagnetic waves propagating making an angle θ with the external magnetic field $\tilde{\mathbf{b}}$. This is equivalent to one of the two geometries [51]: (i) $\overrightarrow{\mathbf{k}}=\hat{\mathbf{e}}_x k$ and $\tilde{\mathbf{b}}=\hat{\mathbf{e}}_x\,B_o\,\cos\theta+\hat{\mathbf{e}}_z\,B_o\,\sin\theta$; (ii) $\tilde{\mathbf{b}}=\hat{\mathbf{e}}_z\,B_o$ and $\overrightarrow{\mathbf{k}}=\hat{\mathbf{e}}_z\,k\,\cos\theta+\hat{\mathbf{e}}_x\,k\,\sin\theta$. In addition, $\theta=0^\circ$ ($\theta=90^\circ$) corresponds to the electromagnetic (EM) mode propagating parallel (perpendicular) to the external magnetic field.

3 Derivation of KdV and KdV Type Equations

To study the nonlinear propagation of the electromagnetic perturbation modes in the proposed ultracold and degenerate EP plasma, we use a weakly nonlinear theory which leads to the scaling of the independent variables as [22]

$$X=\epsilon^{1/2}\left(x-\lambda t\right)\ \text{and}\ T=\epsilon^{3/2}t, \tag{7}$$

where λ is the wave phase speed and ϵ is a measure of the solitary wave amplitude. We now expand the perturbed quantities n, $u_{x,y,z}$, and $b_{y,z}$ about their equilibrium values in powers of ϵ as

$$\begin{aligned}
n &= 1+\epsilon n^{(1)}+\epsilon^2 n^{(2)}+\epsilon^3 n^{(3)}+\ldots,\\
u_x &= \epsilon u_x^{(1)}+\epsilon^2 u_x^{(2)}+\epsilon^3 u_x^{(3)}+\ldots,\\
u_y &= \epsilon^{3/2}u_y^{(1)}+\epsilon^{5/2}u_y^{(2)}+\epsilon^{7/2}u_y^{(3)}+\ldots,\\
u_z &= \epsilon u_z^{(1)}+\epsilon^2 u_z^{(2)}+\epsilon^3 u_z^{(3)}+\ldots,\\
b_x &= \cos\theta,\\
b_y &= \epsilon^{3/2}b_y^{(1)}+\epsilon^{5/2}b_y^{(2)}+\epsilon^{7/2}b_y^{(3)}+\ldots,\\
b_z &= \sin\theta+\epsilon b_z^{(1)}+\epsilon^2 b_z^{(2)}+\epsilon^3 b_z^{(3)}+\ldots.
\end{aligned} \tag{8}$$

To the lowest orders in ϵ, we get

$$n^{(1)}=\frac{b_z^{(1)}\sin\theta}{\alpha_2},\ u_x^{(1)}=\frac{\lambda b_z^{(1)}\sin\theta}{\alpha_2},\ u_z^{(1)}=-\frac{b_z^{(1)}\cos\theta}{\lambda}, \tag{9}$$

where $\alpha_2=\lambda^2-\beta$ and

$$\lambda_{f,s}=\sqrt{\frac{1}{2}\left[(1+\beta)\pm\sqrt{(1+\beta)^2-4\beta\cos^2\theta}\right]}. \tag{10}$$

Equation 10 is the linear dispersion relation which yields two possible electromagnetic wave velocities in the magnetized degenerate EP plasma under consideration; the fast (slow) magnetosonic wave mode velocity λ_f (λ_s) corresponds to + (−) sign. It is noted here that Eq. 10 agrees

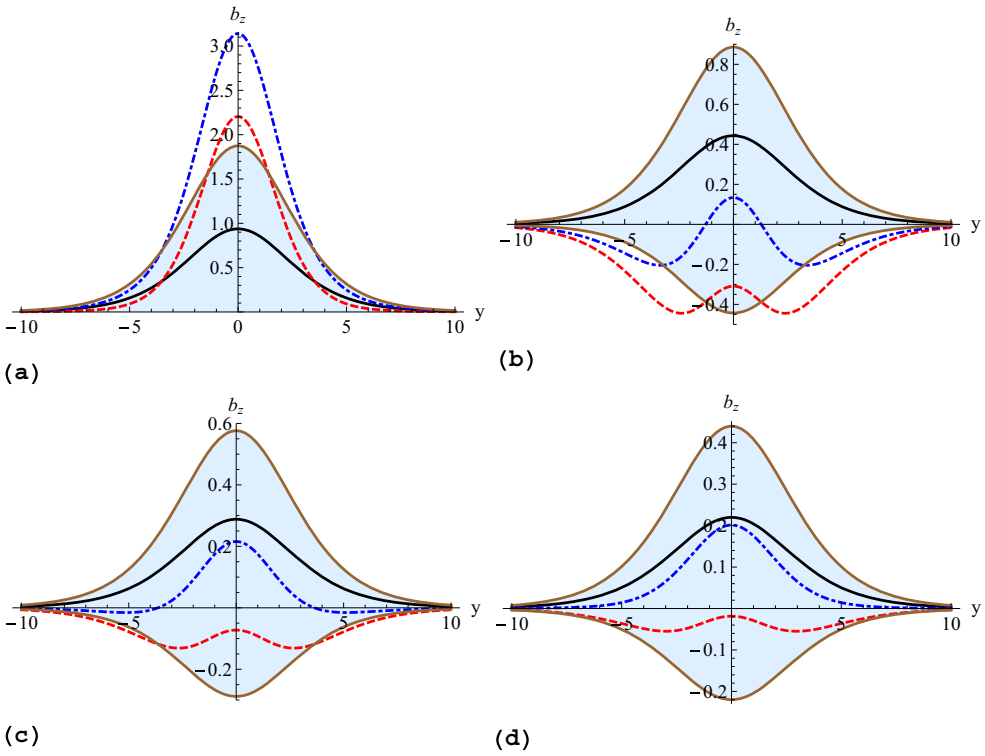

Fig. 1 The fast electromagnetic waves ($\lambda = \lambda_f$), propagating in an EP plasma with $\mu = 1$, $\beta = 1.2$, $u_o = 0.1$. The variations of $b_z^{(1)}$ (*solid black curve*), $b_{zp}^{(2)}$ (*red dashed curve*) and b_z (*dot-dashed blue curve*) are plotted against y. In (**a**) $\theta = 30°$, (**b**) $\theta = 45°$, (**c**) $\theta = 60°$, and (**d**) $\theta = 80°$. Note that the *shaded region* is the region where the solution, b_z, is valid

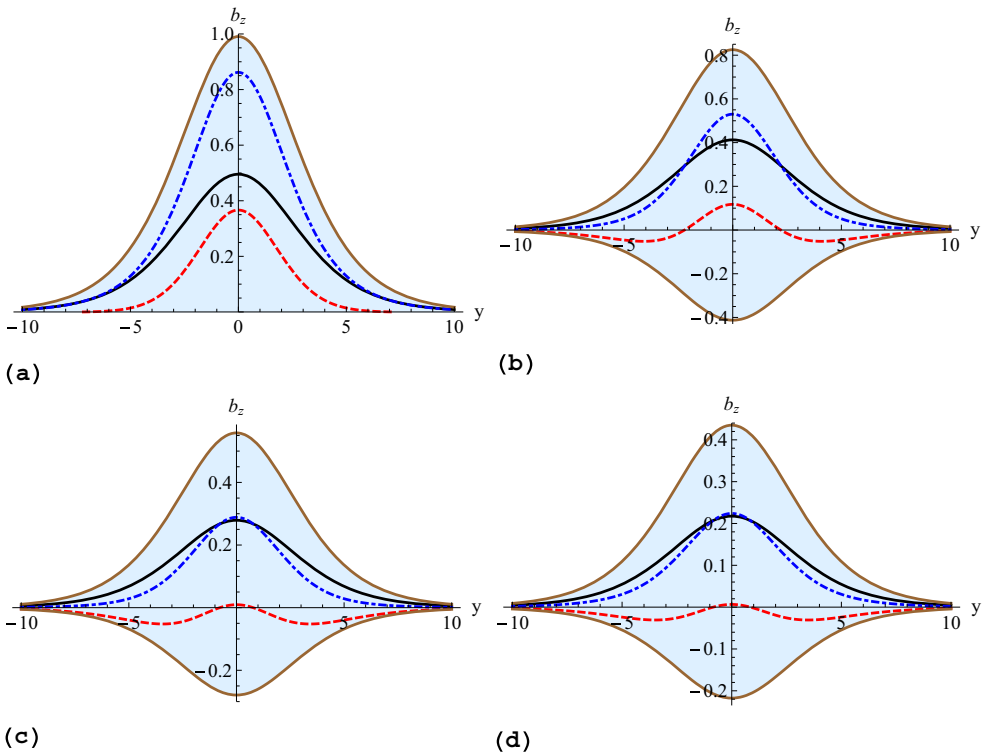

Fig. 2 The fast electromagnetic waves ($\lambda = \lambda_f$), propagating in an EP plasma with $\mu = 1$, $\beta = 0.9$, $u_o = 0.1$. The variations of $b_z^{(1)}$ (*solid black curve*), $b_{zp}^{(2)}$ (*red dashed curve*), and b_z (*dot-dashed blue curve*) are plotted against y. In (**a**) $\theta = 40°$, (**b**) $\theta = 45°$, (**c**) $\theta = 60°$, and (**d**) $\theta = 80°$

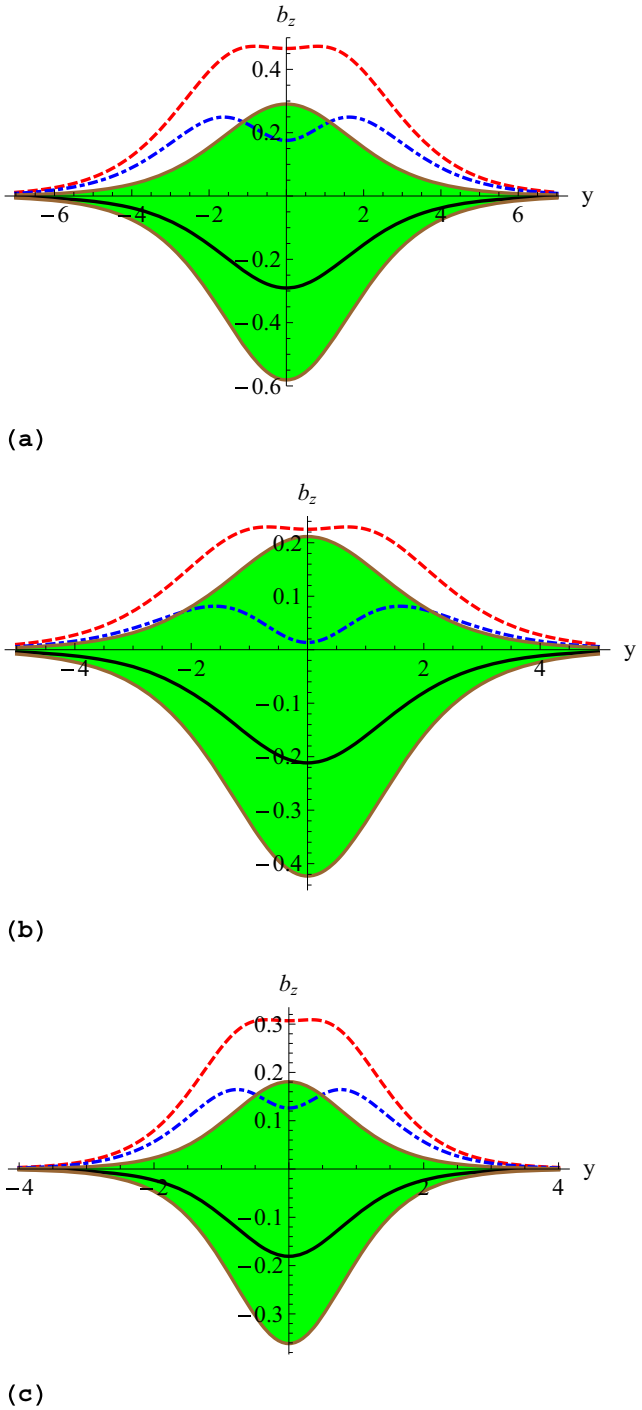

Fig. 3 The slow electromagnetic waves ($\lambda = \lambda_s$), propagating in an EP plasma with $\mu = 1$, $\beta = 1.2$, $u_o = 0.1$. The variations of $b_z^{(1)}$ (*solid black curve*), $b_{zp}^{(2)}$ (*red dashed curve*), and b_z (*dot-dashed blue curve*) are plotted against y. In (**a**) $\theta = 50°$, (**b**) $\theta = 65°$, and (**c**) $\theta = 80°$

exactly with the relation obtained in [18, 52]. Whereas, Mamun et al. [52] employed Fourier linear analysis and a general dispersion relation is obtained. They discussed in details the dispersion properties of parallel and perpendicular propagating electromagnetic waves in EI dense magnetoplasma. Their dispersion relation is split into two, one corresponds to Alfven-like and the other to magneosonic-like wave mode. The next set of the equations, which are obtained by substituting (7) and Eq 8 into Eqs. 1–6 and then equating the coefficients of ϵ^2, leads to

$$u_y^{(1)} = D_\mu \frac{\partial b_z^{(1)}}{\partial X} \text{ and } b_y^{(1)} = \eta \frac{\partial b_z^{(1)}}{\partial X}, \tag{11}$$

where $D_\mu = \mu - \left\{(1-\mu)\cos^2\theta/\nu_1\right\}$, $\eta = \lambda\,(1-\mu)\cos\theta/\nu_1$ and $\nu_1 = \lambda^2 - \cos^2\theta$. For $\mu = 1$, (11) becomes

$$u_y^{(1)} = \frac{\partial b_z^{(1)}}{\partial X} \text{ and } b_y^{(1)} = 0.$$

Therefore, $m_e = m_p$ has a significant role in the expressions of $u_y^{(1)}$ and $b_y^{(1)}$.

Going further in the perturbation theory, considering the coefficients of $\epsilon^{5/2}$ and eliminating the second-order perturbed quantities, we obtain a KdV equation as,

$$\frac{\partial b_z^{(1)}}{\partial T} + A b_z^{(1)} \frac{\partial b_z^{(1)}}{\partial X} + D \frac{\partial^3 b_z^{(1)}}{\partial X^3} = 0, \tag{12}$$

where

$$A = \frac{\lambda}{H_1}\sin\theta\left(3\alpha_2^2 + \frac{8}{3}\beta\sin^2\theta\right),$$

$$D = \frac{\lambda^2\alpha_2}{H_1}\left[\mu\left(\mu - D_\mu\right) + D_\mu\right],$$

with

$$H_1 = \left(\alpha_1\lambda^2\sin^2\theta + \alpha_2^2\nu_2\right)/\left(\alpha_2\lambda\right),$$

$\alpha_1 = \alpha_2 + 2\beta$ and $\nu_2 = \nu_1 + 2\cos^2\theta$. For $\mu = 1$, $D_\mu = 1$, $D > 1$ which allows the existence of solitary wave solutions of Eq 12. Equation 12 agrees exactly with the work of El-Taibany et al. [18]. The stationary soliton solution of Eq. 12 is given by,

$$b_z^{(1)} = b_m\,\mathrm{sech}^2\left(y/\Delta\right) \tag{13}$$

where $y = X - u_\circ T$. The solitary wave amplitude b_m is $3u_\circ/A$, whereas its width Δ is given by $\Delta = 2\sqrt{D/u_\circ}$.

On the other hand, the second-order perturbed quantities $n^{(2)}$, $u_x^{(2)}$, and $u_z^{(2)}$ can be estimated in terms of $b_z^{(1)}$ and $b_z^{(2)}$, with the help of Eqs 9–12, as follows

$$n^{(2)} = \frac{\sin\theta}{\alpha_2}b_z^{(2)} + E\frac{\partial^2 b_z^{(1)}}{\partial X^2} + F{b_z^{(1)}}^2, \tag{14}$$

$$u_x^{(2)} = \frac{\lambda\sin\theta}{\alpha_2}b_z^{(2)} + G\frac{\partial^2 b_z^{(1)}}{\partial X^2} + H{b_z^{(1)}}^2, \tag{15}$$

$$u_z^{(2)} = -\frac{\cos\theta}{\lambda}b_z^{(2)} + I\frac{\partial^2 b_z^{(1)}}{\partial X^2} + \frac{A\cos\theta}{2\lambda}{b_z^{(1)}}^2, \tag{16}$$

where the coefficients E, F, G, H, and I are given in the Appendix. In addition, from the next higher-order

in ϵ, we can calculate the values of $b_y^{(2)}$ and $u_y^{(2)}$ as follows,

$$u_y^{(2)} = D_\mu \frac{\partial b_z^{(2)}}{\partial X} + J\frac{\partial^3 b_z^{(1)}}{\partial X^3} + K b_z^{(1)}\frac{\partial b_z^{(1)}}{\partial X}, \quad (17)$$

$$b_y^{(2)} = \eta\frac{\partial b_z^{(2)}}{\partial X} + L\frac{\partial^3 b_z^{(1)}}{\partial X^3} + M b_z^{(1)}\frac{\partial b_z^{(1)}}{\partial X}, \quad (18)$$

where the values of the coefficients J, K, L, and M are provided in the Appendix.

Equating the coefficients of $\epsilon^{7/2}$in the basic equations, we get,

$$\frac{\partial n^{(2)}}{\partial T} + \frac{\partial}{\partial X}\left(u_x^{(3)} - \lambda n^{(3)} + n^{(1)}u_x^{(2)} + u_x^{(1)}n^{(2)}\right) = 0, \quad (19)$$

$$\frac{\partial u_x^{(2)}}{\partial T} + \frac{\partial}{\partial X}\left(\sin\theta\, b_z^{(3)} - \lambda u_x^{(3)} + \beta n^{(3)} + u_x^{(1)}u_x^{(2)} + b_z^{(1)}b_z^{(2)} - \frac{1}{3}\beta n^{(1)}n^{(2)} + \frac{1}{2}b_y^{(1)^2}\right) + \sin\theta\left(n^{(1)^2}\frac{\partial b_z^{(1)}}{\partial X} - n^{(1)}\frac{\partial b_z^{(2)}}{\partial X} - n^{(2)}\frac{\partial b_z^{(1)}}{\partial X}\right) - n^{(1)}b_z^{(1)}\frac{\partial b_z^{(1)}}{\partial X} + \frac{2}{3}\beta\frac{\partial n^{(1)^3}}{\partial X} = 0, \quad (20)$$

$$\frac{\partial u_z^{(2)}}{\partial T} - \lambda\frac{\partial u_z^{(3)}}{\partial X} + \mu\left[\frac{\partial^2 b_y^{(1)}}{\partial X\partial T} + u_x^{(1)}\frac{\partial^2 b_y^{(1)}}{\partial X^2} + \lambda\left\{\frac{\partial}{\partial X}\left(n^{(1)}\frac{\partial b_y^{(1)}}{\partial X}\right) - \frac{\partial^2 b_y^{(2)}}{\partial X^2}\right\}\right] + \cos\theta\left(-\frac{\partial b_z^{(3)}}{\partial X} + n^{(1)}\frac{\partial b_z^{(2)}}{\partial X} + n^{(2)}\frac{\partial b_z^{(1)}}{\partial X} - n^{(1)^2}\frac{\partial b_z^{(1)}}{\partial X}\right) + u_x^{(1)}\frac{\partial u_z^{(2)}}{\partial X} + u_x^{(2)}\frac{\partial u_z^{(1)}}{\partial X} = 0, \quad (21)$$

$$\frac{\partial b_z^{(2)}}{\partial T} + \frac{\partial}{\partial X}\left[\sin\theta u_x^{(3)} - \cos\theta u_z^{(3)} - \lambda b_z^{(3)} + u_x^{(1)}b_z^{(2)} + u_x^{(2)}b_z^{(1)} - \frac{\partial u_y^{(1)}}{\partial T} - \left(u_x^{(1)}\frac{\partial u_y^{(1)}}{\partial X}\right)\right] + \lambda\frac{\partial^2 u_y^{(2)}}{\partial X^2} = 0. \quad (22)$$

Solving this nonlinear system of partial differential equations; (19)–(22), by eliminating the third-order perturbed quantities, we obtain finally, with the aid of Eqs 9–12, a linear inhomogeneous equation (a KdV type) for the second-order perturbed magnetic field, $b_z^{(2)}$

$$\frac{\partial b_z^{(2)}}{\partial T} + A\frac{\partial}{\partial X}\left(b_z^{(1)}b_z^{(2)}\right) + D\frac{\partial^3 b_z^{(2)}}{\partial X^3} = Q\left(b_z^{(1)}\right), \quad (23)$$

with

$$Q\left(b_z^{(1)}\right) = R_1 b_z^{(1)^2}\frac{\partial b_z^{(1)}}{\partial X} + R_2\frac{\partial b_z^{(1)}}{\partial X}\frac{\partial^2 b_z^{(1)}}{\partial X^2} + R_3 b_z^{(1)}\frac{\partial^3 b_z^{(1)}}{\partial X^3} + R_4\frac{\partial^5 b_z^{(1)}}{\partial X^5}, \quad (24)$$

where R_s ($s = 1, 2, 3, 4, 5$) are given in the Appendix.

Thus, we conclude that the basic set of Eqs. 1–6 is reduced to a KdV equation, (12), for the first-order perturbed magnetic field, $b_z^{(1)}$, and a KdV type equation, (23), for the second-order perturbed magnetic field, $b_z^{(2)}$.

Applying the renormalization method [50, 53] and removing the secular terms, we can finally obtain the higher-order magnetic field soliton solution

$$b_z = b_z^{(1)} + b_{zp}^{(2)} = \left[b_m + \frac{a}{6} + \frac{b}{4} - \frac{b}{8}\,\mathrm{sech}^2\left(y/\Delta\right)\right]\mathrm{sech}^2\left(y/\Delta\right), \quad (25)$$

where $b_{zp}^{(2)}$ is the particular solution of Eq. 23 and

$$a = \frac{18u_o^2}{AD}\left(\frac{R_2+R_3}{A} - \frac{5R_4}{D}\right) \text{ and } b = \frac{36u_o^2}{A}\left(\frac{R_1}{A^2} + \frac{5}{2}\frac{R_4}{D^2} - \frac{R_2+2R_3}{2DA}\right).$$

It is noted here that we omit the details of the renormalization method. For review of the details of this method, please consult for example [47–50, 53].

4 Discussion and conclusion

We have considered a degenerate EP plasma consisting of inertial ultracold electron and positron fluids following the nonrelativistic equation of state $P_j \propto N_j^{5/3}$. The contribution of higher-order nonlinearity and dispersion to the electromagnetic waves propagation in such a degenerate EP plasma system is investigated. We have left the mass ratio parameter, μ, to be arbitrary in order to include an analysis for EI plasma model where $\mu \gg 1$. Using a RPT, the basic set of fluid equations describing the system leads, at the lowest-order of perturbation theory, to KdV equation, Eq. 12, and to inhomogeneous linear KdV type equation, (23), for the higher-order perturbed magnetic field. The higher-order nonlinear and dispersion terms are included in searching for a better accuracy and for new features that may exist. Using the renormalization method [50, 53], the solutions of these coupled evolution equations are obtained, Eqs. 13 and 25.

In the following set of illustrations, let us take the actual parameter values of white dwarfs; $n_o = 10^{25} - 10^{28}\mathrm{cm}^{-3}$and $B_o = 10^7 - 10^9$G, [10, 11, 18, 52, 54–57]. Before going through the numerical illustrations, let us first check the validity of the proposed theoretical model according to the selected white dwarf numerical values. We have neglected the spin effects of electrons and positrons [54] since the (magnetization energy) $\mu_B B_o \ll k_B T_{Fe}$ (Fermi energy) [where μ_B is the Bohr magneton for electron and

defined as $\mu_B = e\hbar/(2m_e c)$] is valid and it holds in our numerical calculations as well. We have calculated the numerical values of the these parameters $\mu_B B_o = 8.5 \times 10^{-12}$ergs [with $B_o = 10^9$ G] and Fermi energy of electrons is $k_B T_{Fe} = 2.76 \times 10^{-8}$ergs [with $T_{Fe} = 2 \times 10^8 K$]. So it is clear that $\mu_B B_o \ll k_B T_{Fe}$.

We assign for the lowest- [higher-] order perturbed magnetic field $b_z^{(1)}[b_{zp}^{(2)}]$ solid black [dashed red] curve; however, the total magnetic field, (25), b_z is presented by a dotted blue curve. The shaded area determines where the higher-order solution evaluated from the RPT is valid. Within this area, the condition $\left|b_{zp}^{(2)}\right| \leqslant \left|b_z^{(1)}\right|$is verified. Some authors concern on the verification of this condition only at $y = 0$; however, we stress it should be satisfied for the whole y-range. Very recently, El-Taibany et al. [18] have shown that the electromagnetic perturbation wave behaviors change drastically around the value $\beta = 1$ (β is a physical parameter proportional to the degenerate plasma pressure

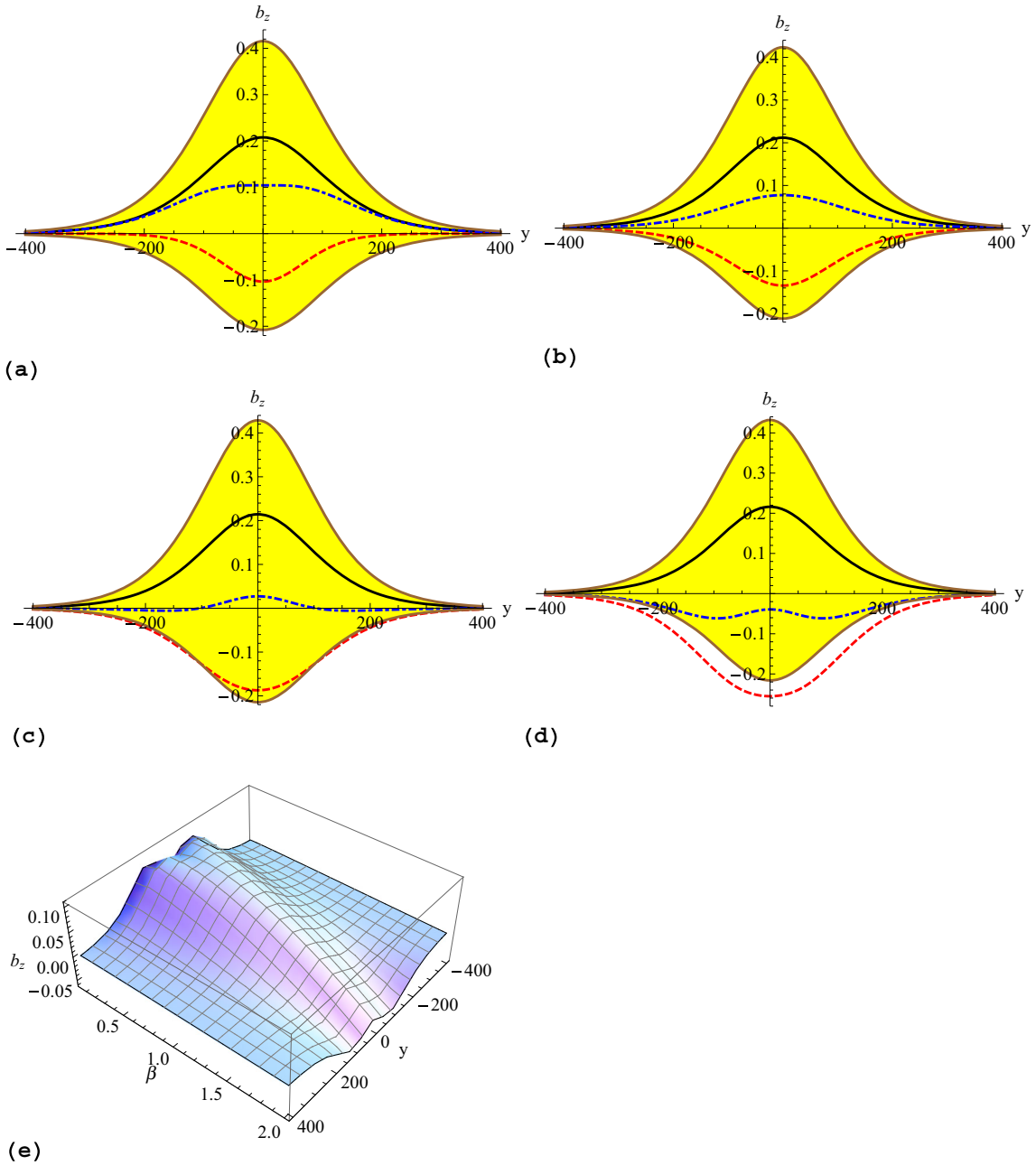

Fig. 4 The fast electromagnetic wave ($\lambda = \lambda_s$), propagating in an EI plasma with $\mu = 1836$, $\theta = 89^o$, $u_o = 0.1$, the variations of $b_z^{(1)}$ (*solid black curve*), $b_{zp}^{(2)}$ (*red dashed curve*), and b_z (*dot-dashed blue curve*) are plotted against y. In (**a**) $\beta = 0.5$, (**b**) $\beta = 1$, (**c**) $\beta = 1.5$, and (**d**) $\beta = 2$. In (**e**), the three-dimensional variation of b_z against β and y

form, it is normalized by V_A^2 and it depends explicitly on the plasma density, n_o, and the magnetic field, B_o). As defined in Section 2, $\beta = 2\hbar c\Lambda_c n_o^{2/3}/\left[V_A^2\left(m_e + m_p\right)\right]$ that can be reformulated to be $\beta = 9.54 \times 10^{-26}\left(n_o^{5/3}/B_o^2\right)$. For instance, let $n_0 = 10^{25}$ cm^{-3} and $B_0 = 10^9$ G, we get $\beta = 0.044$, though the unity β value; $\beta = 1$,corresponds to $n_o = 6.5 \times 10^{25}$ and 10^9 G. Setting 10^{26} cm^{-3}and choosing the same value of $B_o = 10^9$, we obtain $\beta = 2.06$. Therefore, in the following numerical illustrations, we prefer to cover possible wide range of β for two reasons: first, to compare these results with those of Ref. [18] and second, to illustrate the reliable relation of the electromagnetic wave characteristics against the plasma density and the magnetic field strength. In other words, we can say that smaller values of β correspond to small value of n_o or large B_o value; very strong magnetic field and vice versa. In Fig. 1, for a dense EP plasma; $\beta = 1.2$, the variation of the total fast electromagnetic wave (corresponds to λ_f), b_z, is plotted against θ variation in different panels. It is proved that since the soliton wave for the lowest-order perturbed magnetic field, $b_z^{(1)}$, has a compressive character [18], though including the higher-order corrections reveals that it transfers to be a compressive hump with two rarefactive tails for intermediate values of θ; $30^\circ < \theta < 80^\circ$. But when going closer to $\theta = 90^\circ$, b_z returns back to be a pure compressive wave. It is obvious that the RPT can cover fast electromagnetic soliton description where $50^\circ < \theta < 90^\circ$. In Fig. 1a, for $\theta = 30^\circ$, $b_z^{(1)}$ exceeds the equilibrium value of b_z [see b_z expansion in the last equation of (8); $b_z^{(1)} \simeq 0.95$ and $b_{zp}^{(2)} = 2.2$ but $\sin\theta = 0.5$]. Also, the wave amplitudes in this panel exceed the small-wave amplitude limit. In other words, for smaller propagation angle, $\theta < 50^\circ$, the theory cannot describe the produced wave soliton due to verification of the above-mentioned condition, though it could work only for the variation around $y = 0$. Moreover, introducing the higher-order nonlinearity reduces the fast electromagnetic wave amplitude and shrinks its width in such dense and degenerate EP plasma, c.f. Fig. 1 panels (b–d). On the other side, with $\beta = 0.9$, Fig. 2 illustrates the dependence of b_z on θ variation. It is remarked here that, in this case, the total magnetic field, b_z, lies within the verified area, i.e., the RPT works perfectly. In addition, b_z has a compressive feature similar to $b_z^{(1)}$ produced by El-Taibany et al. [18]. For $\theta \leqslant (> 45^\circ)$, the amplitude of b_z increases (slightly increases), though its width becomes narrower for any value of θ. Figure 3 is devoted to illustrate the variation of the slow electromagnetic wave, b_z, (corresponding to λ_s), against θ changes. In this case, incorporating the higher-order nonlinear terms results in inverting the slow electromagnetic wave dip to be a two-hump compressive soliton. The RPT restriction yields that the theory can describe the whole slow electromagnetic soliton corresponding to $\beta = 1.2$ within a very small range of θ; $65^\circ < \theta < 70^\circ$ and partially (just around $y = 0$) for $50^\circ < \theta < 65^\circ$ and $70^\circ < \theta < 80^\circ$. However, for $\beta \leqslant 1$, the RPT cannot work for this slow mode in EP plasma (not shown here). Generally, the amplitude of the soliton wave is reduced as well as its width. Comparing among Fig. 3 panels, one can observe that, by increasing the value of θ, the magnetic field soliton appears within a smaller y-range; the soliton structure is shrunk.

Now, let us examine the case of an EI degenerate dense plasma model (setting $\mu = 1836$) that appeared as Fig. 4 with $\lambda = \lambda_f$. It should be mentioned here that to verify the degeneracy state of ion species in the case of EI plasma, the following condition (Fermi temperature of ions) $T_{Fi} \gg T$ (thermal temperature) is satisfied. The degeneracy related parameter is defined as $\chi_j = T_{Fj}/T$ (where $j = e$, p, or i). Therefore, $\chi_j \gg 1$ for both of electrons and ions [using $T_{Fe} = 2 \times 10^8 K$ and $T_{Fi} = 8 \times 10^7 K$ as the Fermi temperature for electrons and ions, respectively]. On the other side, the Coulomb coupling parameter for ions is defined as $\Gamma = e^2/(k_B T d)$ where $d = (3/4\pi n_o)^{1/3}$ is the mean interionic distance. Using $T = 2 \times 10^7$ K and $n_o = 10^{27}$ cm^{-3}, we have $\Gamma = 0.029 \ll 1$ [55]. Thus, we can assume that the correlations among ions (i.e., the ion crystallization effect) are ignored in the proposed fluid model of dense plasma. Figure 4 elucidates that the b_z soliton becomes wider with an amplitude smaller than that of $b_z^{(1)}$, due to the introduction of the higher-order nonlinear and dispersion terms. In addition, b_z is firstly a two-hump soliton structure corresponding to very small β value, then becomes a wider compressive soliton (at moderate β value) then finally for higher values of β, it becomes two-dip rarefactive (W-shaped) soliton with smaller amplitude and narrower width, c.f. Fig. 4d. As discussed in El-Taibany et al. [18], the present results would be applied to an EI plasma model (last case) by satisfying the following condition

$$\mu < \lambda^2 \sec^2\theta - 1, \tag{26}$$

which corresponds to a positive value of the dispersion coefficient, D. According to Eq. 26, θ should be very close to 90°. Since El-Taibany et al. [18] proved that the fast electromagnetic perturbed magnetic field wave, $b_z^{(1)}$, is a compressive soliton, b_z changes its feature from compressive ($\beta < 1$) to rarefactive at $\beta > 1$. Although the RPT cannot provide a description for the soliton which corresponds to the slow wave velocity, λ_s. It is noted from Eq. 10, λ_s corresponds to the negative sign. Therefore, the wave velocity as well as the produced soliton wave are very sensitive to θ and β variations.

To conclude, it is important to incorporate the higher-order nonlinear corrections; however, the RPT cannot work perfectly for all nonlinear electromagnetic wave domain in either EP or EI dense and degenerate plasma. We can summarize the effects of these corrections as follows:

1. In EP dense plasma ($\mu = 1$), for the fast wave ($\lambda = \lambda_f$), it reduces (increases) the soliton amplitude corresponding to $\beta > 1 (< 1)$; however, its width decreases for any value of β. For $\beta < 1$, the final soliton type is compressive; for $\beta > 1$ it is also a compressive soliton, with rarefactive tail appearing at moderate θ and disappearing for increasing θ. Moreover, the RPT can work for the whole θ variation with $\beta < 1$ but for $\beta > 1$, it could be used for $50^\circ < \theta < 90^\circ$ only.
2. In EP dense plasma ($\mu = 1$), for the slow wave ($\lambda = \lambda_s$), it contributes in changing the soliton from a rarefactive dip structure to a two-humped compressive one, with similar amplitude but with reduced width. The RPT is working for very small range of the propagation angle, $65^\circ < \theta < 70^\circ$ with $\beta > 1$. Otherwise, it cannot be employed.
3. For EI dense plasma ($\mu = 1836$), for the fast wave ($\lambda = \lambda_f$), it changes the soliton structure from two-hump (at very small β value), passing through a wider compressive soliton (moderate β values) and finally at higher β value it becomes two-dip rarefactive soliton (W-shaped soliton). The RPT works perfectly for these fast modes where θ is very close to the perpendicular direction, i.e., $\theta \simeq 90^\circ$. Whereas it can not be used for the slow wave modes.
4. Finally, we stress that one must be careful when applying the RPT in studying obliquely propagating electromagnetic waves in either EI or EP plasma. We suggest to employ a non-perturbative technique or numerical simulation method where RPT cannot work. The present findings due to incorporation of these higher-order corrections show significant modifications on the basic properties of the solitary wave solutions (polarity, amplitude, and width), and revealing new features in comparison between EP and EI plasmas.

Our present investigation would be helpful in understanding the basic features of the localized electromagnetic disturbances in compact astrophysical objects, e.g., white dwarf stars, which are used as appropriate application [35–43]. It may be added that the effects of inhomogeneity in plasma density and ambient magnetic field on these electromagnetic solitary structures and their stability analysis are also problems of great importance, but this is beyond the scope of the present work.

Appendix

The expressions of the coefficients appeared in Eqs. 14–16 are

$$E = -\frac{2D\lambda\sin\theta}{\alpha_2^2},\ F = \frac{1}{2\alpha_2} - \frac{A\lambda\sin\theta}{\alpha_2^2} + \frac{\sin^2\theta}{2\alpha_2^3}\left(3\lambda^2 - \alpha_2 - \frac{\beta}{3}\right),$$

$$G = E\lambda + \frac{D\sin\theta}{\alpha_2},\ H = F\lambda - \frac{\lambda\sin^2\theta}{\alpha_2^2} + \frac{A\sin\theta}{2\alpha_2},$$

$$I = \cos\theta\left[\frac{D}{\lambda^2} - \frac{\mu\lambda(1-\mu)}{\alpha_2}\right].$$

The expressions of those presented in Eqs. 17 and 18 are

$$J = \frac{(\mu - D_\mu)D - L\cos\theta}{\lambda},\ K = \frac{[(\mu - D_\mu)A - M\cos\theta]}{\lambda} - \frac{\mu\sin\theta}{\alpha_2},$$

$$L = \frac{\eta}{\lambda}\left[\frac{\mu\lambda^3}{\alpha_2} - \frac{D\nu_2}{\nu_1}\right],\ M = -\frac{\eta}{\nu_1}\left[\frac{A\nu_2}{\lambda} - \frac{\sin\theta\cos^2\theta}{\alpha_2}\right].$$

Finally, the coefficients appeared within the source term, (24), are

$$R_1 = -\frac{1}{H_1}\left[\left(\sin^2\theta/\alpha_2\right)\left(\cos^2\theta + \lambda^2\left\{-1 + \left(\sin^2\theta/\alpha_2\right) + \left[2\sin^2\theta/\left(9\beta\alpha_2^2\right)\right]\right\}\right) - (A/\lambda)\sin\theta\cos^2\theta + F\left\{\beta\left[\cos^2\theta + 2\left(\lambda^2/\alpha_2\right)\sin^2\theta\right] - \lambda^2\right\} + H\left[(\alpha_2/\lambda)\left(3\lambda^2 + \cos^2\theta\right) + 3\left(\alpha_1/\alpha_2\right)\lambda\sin^2\theta\right]\right],$$

$$R_2 = -\frac{1}{H_1}\left\{3\alpha_2\lambda\left(K\lambda + M\mu\cos\theta\right) - \lambda^2\sin\theta\left[\mu^2 - \eta^2 + D_\mu(1-\mu)\right] + E\left(\beta\left\{\cos^2\theta + 2\left[\left(\lambda^2\sin^2\theta\right)/(3\alpha_2)\right]\right\} - \lambda^2\right)\right\},$$

$$R_3 = -\frac{1}{H_1}\left\{\alpha_2\lambda\left(\lambda K + M\mu\cos\theta\right) - \lambda^2\sin\theta\left[2\mu^2 + D_\mu(1-2\mu)\right] + G\lambda\left[\alpha_2 + (\alpha_1/\alpha_2)\sin^2\theta\right] + [2/(3\alpha_2)]\,E\beta\lambda^2\sin^2\theta - \lambda I\sin\theta\cos\theta\right\},$$

$$R_4 = -\frac{\alpha_2\lambda}{H_1}\left(\lambda J + \mu L\cos\theta\right),$$

References

1. D. Bohm, D. Pines. Phys. Rev. **92**, 609 (1953)
2. D. Pines. Phys. Rev. **92**(626) (1953)
3. P. Levine, O.V. Roos. Phys. Rev. **125**, 207 (1962)
4. L.D. Landau, E.M. Lifshitz, *Statistical physics Part I* (Pergamon, Oxford, 1978)
5. H. Haug, S.W. Koch, *Quantum theory of the optical and electronic properties of semiconductors* (World Scientific, London, 2004)

6. P.K. Shukla, B. Eliasson. Rev. Mod. Phys. **83**, 885 (2011)
7. F. Haas, Quantum plasmas: An hydrodynamic approach. (Springer Series on atomic, optical, and plasma physics 65, New York, 2011).
8. S. Chandrasekhar. Mon. Not. R. Astron. Soc. **95**(81), 207 (1935)
9. L. Shapiro, S.A. Teukolsky, *Black holes, white dwarfs, neutron stars: the physics of compact objects* (John Wiley and Sons, New York, 1973)
10. D. Koester, G. Chanmugam. Rep. Prog. Phys. **53**, 837 (1990)
11. P.A. Bradley, P.E. Winget, M.A. Wood. Astrophys. J. **406**, 661 (1993)
12. G.A. Mourou, T. Tajima, S.V. Bulanov. Rev. Mod. Phys. **78**, 309 (2006)
13. W.F. El-Taibany, M. Wadati. Phys. Plasmas **14**, 042302 (2007)
14. S. Mahmood, S. Sadiq, Q. Haque. Phys. Plasmas **20**, 122305 (2013)
15. M. Akbari-Moghanjoughi. Phys. Plasmas **17**, 092304 (2010)
16. P.K. Shukla, B. Eliasson, L. Stenflo. Phys. Rev. E **84**, 037401 (2011)
17. W.F. El-Taibany, A.A. Mamun. Phys. Rev. E **85**, 026406 (2012)
18. W.F. El-Taibany, A.A. Mamun, Kh. H. El-Shorbagy. Adv. Space Res. **50**, 101 (2012)
19. L. Nahar, M.S. Zobaer, N. Roy, A.A. Mamun. Phys. Plasmas **20**, 022304 (2013)
20. M.A. Hossen, M.R. Hossen, A.A. Mamun. J. Korean Phys. Soc. **65**, 1883 (2014)
21. M.R. Hossen, A.A. Mamun, Braz. J. Phys. (2015) doi:10.1007/s13538-014-0297-4
22. H. Washimi, T. Taniuti. Phys. Rev. Lett. **17**, 996 (1966)
23. L. Stenflo, P.K. Shukla, M.Y. Yu. Astrophys. Space Sci. **117**, 303 (1985)
24. F.B. Rizzato. J. Plasma Phys. **40**, 289 (1988)
25. N.L. Shatashvili, J.I. Javakhishvili, H. Kaya. Astrophys. Space Sci. **250**, 109 (1997)
26. N.L. Shatashvili, N.N. Rao. Phys. Plasmas **6**, 66 (1999)
27. C.M. Surko, M. Levethal, W.S. Crane, A. Passner, F. Wysocki. Rev. Sci. Instrum. **57**, 1862 (1986)
28. M.D. Tinkle, R.G. Greaves, C.M. Surko, R.L. Spencer, G.W. Mason. Phys. Rev. Lett **72**, 352 (1994)
29. G. Gahn, G.D. Tsakiris, G. Pretzler, K.J. Witte, C. Delfin, C.-G. Wahlström, D. Habs. Appl. Phys. Lett. **77**, 2662 (2000)
30. T. Piran. Phys. Rep. **314**, 575 (1999)
31. E. Tandberg-Hansen, A.G. Emslie, *The Physics of Solar Flares* (Cambridge University Press Cambridge, 1988)
32. S.I. Popel, S.V. Vladimirov, P.K. Shukla. Phys. Plasmas **2**, 716 (1995)
33. S.A. Khan, M.K. Ayub, A. Ahmad. Phys. Plasmas **19**, 102104 (2012)
34. S.A. Khan, M. Ilyas, Z. Wazir, Z. Ehsan. Astrophys. Space Sci. **352**, 559 (2014)
35. O. Andriani et al. PAMELA Collaboration, Nature **458**, 607 (2008)
36. O. Adriani, et al., PAMELA collaboration. Astropart. Phys. **34**, 1 (2010)
37. O. Adriani, et al., PAMELA collaboration. Phys. Rev. Lett. **106**, 201101 (2011)
38. O. Adriani, et al., PAMELA collaboration. Phys. Rev. Lett. **111**, 081102 (2013)
39. A.A. Abdo et al., Fermi LAT Collaboration. Phys. Rev. Lett **102**, 181101 (2009)
40. M. Ackermann, Fermi LAT Collaboration. Phys. Rev. D **82**, 092004 (2010)
41. K. Kashiyama, K. Ioka. AIP Conf. Proc. **1279**, 352 (2010)
42. K. Kashiyama, K. Ioka, N. Kawanaka. Phys. Rev. D **83**, 023002 (2011)
43. P.D. Serpico. Astropart. Phys. **39**, 2 (2012)
44. R.S. Tiwari, M.K. Mishra. Phys. Plasmas **13**, 062112 (2006)
45. R.S. Tiwari, A. Kaushik, M.K. Mishra. Phys. Lett. A **365**, 335 (2007)
46. A. Esfandyari-Kalejahi, M. Akbari-Moghanjoughi, B. Haddadpour-Khiaban. Phys. Plasmas **16**, 102302 (2009)
47. P. Chatterjee, K. Roy, G. Mondal, S.V. Muniandy, S.L. Yap, C.S. Wong. Phys. Plasmas **16**, 122112 (2009)
48. M. Akbari-Moghanjoughi. Phys. Plasmas **17**, 052302 (2010)
49. M. Mehdipoor, A. Esfandyari-Kalejahi. Astrophys. Space Sci. **342**, 93 (2012)
50. Y. Kodama, T. Taniuti. Phys, J. Soc. Jpn. **45**, 298 (1978)
51. A.A. Mamun, P.K. Shukla, D.A. Mendis. J. Plasma Phys. **78**, 143 (2012)
52. A.A. Mamun, N. Roy, P.K. Shukla. J. Plasma Phys. **78**, 683 (2012)
53. S.K. El-Labany. J. Plasma Phys. **50**, 495 (1993)
54. S. Hussain, S. Mahmood, A. Pasqua. Phys. Lett. **377**, 2105 (2013)
55. S. Sadiq, S. Mahmood, Q. Haque, M.Z. Ali. Astrophys. J. **793**, 27 (2014)
56. H.M. Van Horn. Phys. Today **32**, 23 (1979)
57. W. Masood, A. Mushtaq. Phys. Lett. A **372**, 4283 (2008)